

A TEMPERATURE-MAPPING SYSTEM FOR MULTI-CELL SRF ACCELERATING CAVITIES*

M. Ge, G. Hoffstaetter, F. Furuta, E. Smith, M. Liepe, S. Posen, H. Padamsee, D. Hartill, X. Mi, Cornell University, Ithaca, NY 14850, USA.

Abstract

A Temperature mapping (T-map) system for Superconducting Radio Frequency (SRF) cavities consists of a thermometer array positioned precisely on an exterior cavity wall, capable of detecting small increases in temperature; therefore it is a powerful tool for research on the quality factor (Q_0) of SRF cavities. A new multi-cell T-mapping system has been developed at Cornell University. The system has nearly two thousand thermometers to cover 7-cell SRF cavities for Cornell's ERL project. A 1mK resolution of the temperature increase ΔT is achieved. A 9-cell cavity of TESLA geometry was tested with the T-map system.

INTRODUCTION

The quality factor (Q_0) of Superconducting Radio Frequency (SRF) cavities is a critical topic in the SRF field. High-Q cavities are able to save cryogenic capacities of accelerators. The definition of Q_0 is given by equation (1), where ω is the angular frequency of the cavity, U is its stored energy, P_{loss} is the power loss on the cavity surface. The Q_0 -value ranks the cavity's efficiency. If we define a geometry factor (G) as function (2), the Q_0 may be written as the ratio of the geometry factor and the surface resistance (R_s).

$$Q_0 = \frac{\omega U}{P_{loss}} = \frac{G}{R_s} \quad (1)$$

$$G = \frac{\omega \mu_0 \int_V |\vec{H}|^2 dV}{\int_A |\vec{H}|^2 dA} \quad (2)$$

The geometry factor is a constant determined by cavity geometry shapes, thus the Q_0 is dictated by cavity surface-resistance.

The T-map system, a thermometer array uniformly attached on a cavity exterior surface, is a powerful tool for surface resistance research. It is able to detect tiny heating on cavity wall during feeding RF power into cavity. Hence by the heating map of whole cavity, it is possible to calculate power loss and surface resistance, furthermore to calculate the Q_0 -value of the cavity. The Q_0 of a multi-cell SRF cavity measured from RF is derived from the total value of all cells. The relationship between total Q_0 of a 9-cell cavity and Q_0 -value of each cell at pi-mode is given by equation (3)

$$\frac{1}{Q_0^{tot}} = \frac{1}{n} \sum_{n=1}^9 \frac{1}{Q_n^{cell}} \quad (3)$$

*This work has been supported by NSF award PHY-0969959 and DOE award DOE/SC00008431

Here Q_0^{tot} is total Q_0 of a 9-cell cavity, and Q_n^{tot} is Q_0 of cell n . The total Q_0 is unable to reflect which cell has low- Q and degrades the whole cavity. However, T-map can diagnose the Q_0 -value of each cell by summing each cell's power loss. Hence T-map gives more information about cavity performance than RF measurement alone.

T-mapping history can be traced back to the 1980s. Cornell University was a pioneer in developing a 1-cell T-map system for 1.5GHz SRF cavity research [1, 2, and 3]. Now Jefferson Lab and Fermilab also have 1-cell or 2-cell T-map systems. These systems are used for fundamental SRF research via single-cell cavities. Therefore the development of a multi-cell T-mapping system is necessary and ultra-important. DESY and Los Alamos have multi-cell T-mapping systems for ILC 9-cell cavities [4, 5]. Those systems are mainly used to detect quench location.

TEMPERATURE-MAPPING SYSTEM DESCRIPTION

This multi-cell T-mapping system has been developed for the Cornell ERL project which requires the Q_0 -value of 7-cell cavities to achieve 2×10^{10} at accelerating gradient 16MV/m [6]. For a 1.3GHz SRF cavity, the heating from RF causes on average about a 10mK temperature rise on the exterior wall at 25MV/m in a 2K helium bath [7]. Thus the resolution of this T-map is required to be approximately 1mK.

Thermometers and Boards

The Cornell multi-cell T-map has nearly two thousand thermometers. The temperature sensor is a 100Ω carbon Allen-Bradley resistor (5% 1/8 W). Carbon is a semiconductor, its resistance increases exponentially when temperature drops. Figure 1 (a) shows the schematic of sensor and its picture. APIEZON grease was applied on the varnished side of the thermometers prior to inserting the boards in cages. The sensor is able to detect the temperature rise of the cavity wall with 25% efficiency [3]. Two sets of 3-cell boards and one set of 1-cell boards were used for 7-cell SRF cavity. A 3-cell board has two channels addressed to the sensors for 3-cells. The sensor boards are spaced azimuthally every 15° around the cavity; totally it has 24 boards around the azimuth. Each cell is covered by an 11×24 thermometer array. Figure 1 (b) shows a 3-cell and a 1-cell board. The quantity of thermometers for the whole 7-cell cavity is 1848. Cornell constructed a new test insert for hanging the multi-cell cavity with full T-map. In Figure 1 (c) the left image shows the Cornell multi-cell T-map attached on middle 7-cells of a 1.3GHz 9-cell cavity; the right image is a picture showing several boards removed to expose the cavity. The

insert has a feedthrough on the top-plate for extracting T-mapping cables out of the Dewar. A coupler motor and Ion pump were built on the insert as well, which allows us to adjust the coupler position as well as to keep the cavity under high-vacuum during the RF test. Three well-calibrated Cernox thermometers were attached on the insert for T-map calibration.

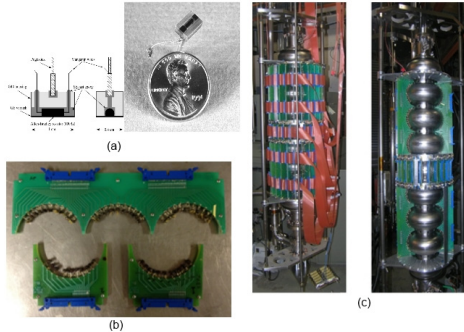


Figure 1: (a) Thermometer schematic, (b) T-map boards, (c) T-map insert.

CRYOGENIC TEST

We tested a 1.3GHz 9-cell cavity which is TESLA shape with the T-mapping system. The cavity was vertically electro-polished about 5 μ m, followed by high pressure water rinsing and clean assembly in a class 10 clean room. No 120 $^{\circ}$ C baking was applied on the cavity.

Calibration and Sensitivity

A well-calibrated Lakeshore Cernox thermometer is utilized as a temperature reference for the helium bath during cooling down from 4.2K to 1.6K. Figure 2 (a) is a sensor's calibration curve.

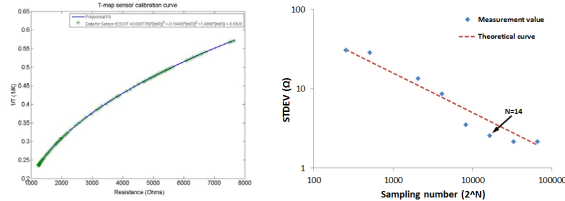


Figure 2 (a): 1/T vs. resistance curve during cooling down, (b) standard deviation vs. sampling number.

A polynomial function was adopted to fit the curve, shown in equation (4).

$$\frac{1}{T} = a_n x^3 + b_n x^2 + c_n x + d_n \quad (4)$$

$$x = \ln(R)$$

Here T is the bath temperature, R is the resistance of the carbon resistor, a_n , b_n , c_n and d_n are fitting parameters for sensor n . By using fitting curves, it is possible to calculate $\frac{dR}{dT}$ which represents the sensitivity of each T-mapping sensor. An Allen-Bradley resistor value is about 12k Ω at 1.6K, $\frac{dR}{dT}$ is approximately 30 Ω /mK; and $\frac{dR}{dT}$ is about 10 Ω /mK at 2K.

Noise comes from the environment and the electronic system. Increasing measurement sampling number is an effective way to reduce noise from the electronic system.

The PIXI controller can sample the sensor voltages at a 500 KHz rate, and average readings for 2^N samples. Figure 2 (b) shows the standard deviation of resistance decreasing with increasing sampling number. The dash line in the plot is a theoretical curve which is the standard deviation versus $\sqrt{1/2^N}$. The standard deviation is reduced to about 2 Ω , when N is set to 14, corresponding to a sampling number of about 16000. We don't choose a higher N value because higher N will significantly extend scan time. The noise from the electronic system is about 200 μ K in a 2K helium bath; and 67 μ K in 1.6K helium. The total scan time is about 100s.

Thermal conductivity of grease as well as press-force of sensor against cavity-wall affects T-map noise level as well. Figure 3 is a lateral view of the subtraction between two T-map scans without applying RF field in 2K Helium bath. The total noise of the T-map system is about 1mK which achieved our initial goal.

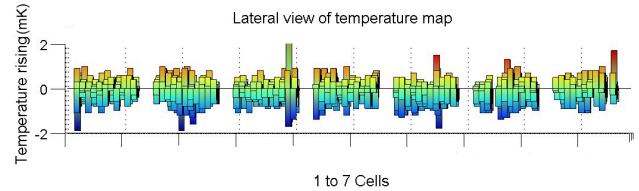


Figure 3: 3-sigma noise level of T-map system. The one sigma noise is only about 0.2mK.

Testing Results of T-map

The 9-cell cavity A9 was tested in a 2K helium bath and quenched at 21MV/m in pi-mode. The T-mapping boards covered the middle 7 cells of the cavity. Temperature-map data was taken at an accelerating gradient very close to quench. Figure 4 (a) depicts the temperature-rise (ΔT) map.

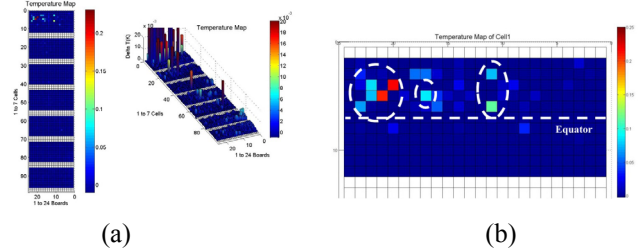


Figure 4: (a) Map of temperature increase for 7-cells of an ILC cavity, (b) Detail T-map view of the dominantly heated Cell 1.

Most heating-spots were found on the top cell which is the top second cell of the 9-cell cavity. The highest ΔT is about 0.2K.

Figure 5 is the summary of ΔT versus H^2 curves; the axis on the right is the Q_0 of the cavity. Equation (5) depicts the ΔT and H^2 relationship of the sensor n . Here R_{sn} is the surface resistance close to the sensor n , \vec{H}_n is the surface magnetic field at the sensor n , as the T-map sensors only cover the high magnetic-field region of each cell, thus $\vec{H}_n \approx H_{peak}$.

$$\Delta T_n = \frac{1}{2C} R_{sn} \vec{H}_n^2 \quad (5)$$

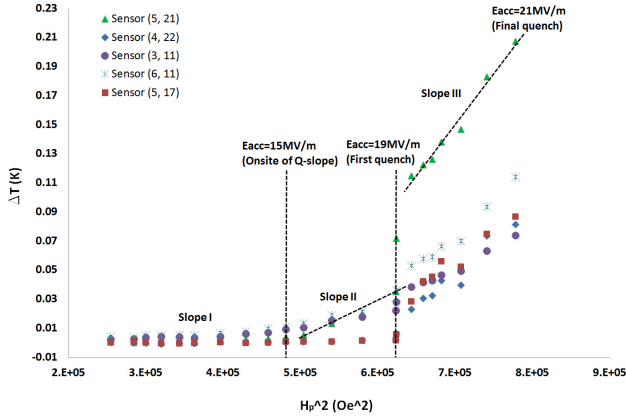


Figure 5: ΔT vs. H^2 curve.

The slopes of ΔT versus H^2 curves indicate R_s at the sensors from equation (5). Three slopes were observed. The slope I started from an acceleration gradient from 0 to 15MV/m. The surface resistance was consisted by BCS resistance and residual resistance. The slope II started at an accelerating gradient (E_{acc}) 15MV/m where the onset of Q-slope is. The surface resistance was increased due to the Q-slope. The heating increased dramatically around 19MV/m at the Multipacting barrier of the TESLA-shape cavity. The Multipacting triggered the first quench and processing of the cavity. After the Multipacting had been processed out, the heating increased with H^2 by the slope III until hard quench (21MV/m). The slope III indicates the surface resistance was increased further by flux trapping after the first quench.

Converting ΔT to Power Loss and Quality Factor

By summing the temperature rising of individual cells, we obtain power loss and quality factor of cavity and each cavity cell, shown in Figure 6 (a) and (b).

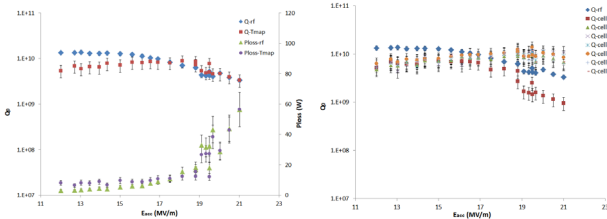


Figure 6 (a): Q_0 , P_{loss} comparison between calculated from T-map and measured from RF. (b) The quality factor of individual cells compared to total Q_0 .

The measurement curves match the calculated curve when the accelerating gradient is higher than 15MV/m where the heating started. Below 15MV/m, the heating from the cavity is too small to be detected accurately. The results from T-map indicate the measured cell 1 generated the most power loss on the surface, and degraded the total Q_0 starting from 15MV/m. The equation (3) suggests that the total Q_0 of the cavity is limited by the Q-value of the

worst cell. The cavity test results also indicate that the Q-slope is possible to be a localized effect.

Surface Resistance Map

A surface resistance map is calculated from the ΔT of each thermometer, which is given by equation (6).

$$R_{sn} = \frac{2C\Delta T_n}{H_{peak}^2} \quad (6)$$

Figure 7 shows a surface resistance map when the cavity was at 21MV/m, close to quench.

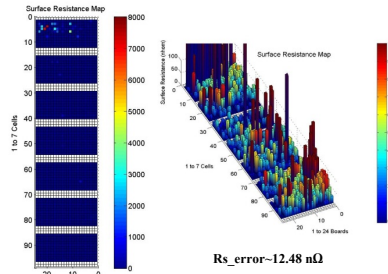


Figure 7: Map of the surface resistance R_s .

The maximum R_s value is close to 8000nΩ, and the average value of all R_s map is 74.26nΩ which agrees with the value (80.84nΩ) calculated from equation (1) by using the geometry factor and Q_0 . The error of the surface resistance is about 16.8% calculated from the measurement error of ΔT , accelerating gradient (E_{acc}) and Q-value by uncertainty propagation formulas.

REFERENCES

- [1] H. Padamsee, et al., “Field Emission Studies in Superconducting Cavities,” PAC’89, Washington D.C., p. 1824 (1989).
- [2] P. Kneisel, G. Mueller and C.Reece, “Investigation of the Surface Resistivity of Superconducting Niobium Using Thermometry in Superfluid Helium,” 1986 Applied Superconductivity Conf., Baltimore, MD.
- [3] J. Knobloch, Ph. D. thesis, CLNS THESIS 97-3(1997). <http://www.lns.cornell.edu/public/CESR/SRF/dissertations/knobloch/knobloch.html>
- [4] Q.S. Shu *et al.*, “An Advanced Rotating T-R Mapping & It’s Diagnoses of TESLA 9-Cell Superconducting Cavity,” PAC’95, Dallas, TX, p. 1639 (1995).
- [5] A. Canabal *et al.*, “Development of a Temperature Mapping system for 1.3-GHz 9-Cell SRF Cavities,” PAC’07, Albuquerque, NM, p. 2406 (2007).
- [6] M. Liepe *et al.*, “Progress on Superconducting RF Work for the Cornell ERL,” IPAC 2012, WEPAC073, (2012).
- [7] Y. Xie, “Relationship between Defects Pre-Heating and Defects Size,” SRF2009, TUPPO049, p. 334, (2009).